https://doi.org/10.5194/hess-2024-395
Preprint. Discussion started: 20 December 2024

Hydrology and Earth System Sciences
Open Access
Discussions

Gypsum as a potential tracer of earthquake: a case study of the *Mw*7.8 earthquake in the East Anatolian Fault Zone, southeastern Turkey

Zebin Luo[1], Xiaocheng Zhou[2,3★], Yueren Xu[2], Peng Liang[2], Huiping Zhang[4], Jinlong Liang[5], Zhaojun Zeng[2], Yucong Yan[3], Zheng Gong[6], Shiguang Wang[6], Chuanyou Li[4], Zhikun Ren[4], Jingxing Yu[4], Zifa Ma[4], Junjie Li[4]

[1]*School of Emergency Management, Xihua University, Chengdu 610039, China*

[2]*United Laboratory of High-Pressure Physics and Earthquake Science, institute of earthquake forecasting, CEA, Beijing 100036, China*

[3]*School of Earth Sciences and Resources, China University of Geosciences, Beijing 100083, China*

[4]*Institute of Geology, China Earthquake Administration, Beijing, 100081, China*

[5]*College of Earth and Planetary Sciences, Chengdu University of Technology, Chengdu 610059, China*

[6] *Institute of Geophysics, China Earthquake Administration, Beijing, 100081, China*

[*] Corresponding author: Xiaocheng Zhou (zhouxiaocheng188@163.com).

Key point:

1. EAFZ geothermal fluid is obviously modified by earthquake, including: energy and materials.

2. EAFZ geothermal fluid is heavily diluted by the infiltration of a large amount of shallow cold water.

3. Shallow sedimentary minerals (e.g., gypsum) could be used as precursory anomaly indicators of earthquakes .

★ Corresponding author

E-mail Address: *Xiaocheng Zhou (zhouxiaocheng188@163.com)*

https://doi.org/10.5194/hess-2024-395
Preprint. Discussion started: 20 December 2024

Hydrology and Earth System Sciences
Discussions

Abstract:

Obvious macroscopic anomalies of geothermal fluids were observed before and after the *Mw* 7.8 earthquake in Turkey. In order to find out the relationship between geothermal fluid anomalies and earthquakes, we performed a systematic hydrogeochemistry and isotopic analysis of the geothermal fluids in the East Anatolian Fault Zone (EAFZ). The results show that these geothermal fluids were reconstructed (including: energy and materials) by earthquakes. Based on chlorine – enthalpy model, the temperature of the deep geothermal fluid has been increasing to 382 ºC on the strength of the energy released by the seismic activity. However, the information of the deep geothermal fluid was eventually covered due to the infiltration of a large amount of shallow cold water after the earthquake. The abnormal concentrations of Ca^{2+} (54.04~501.58mg/L), Mg^{2+} (6.58~116.20mg/L), SO_4^{2-} (6.37~287.74mg/L), Sr (34.78~3244.8μg/L), and Ba (1.89~196.48μg/L) in geothermal water shown that the geothermal water has undergone complex water-rock interaction processes such as gypsum, calcite, dolomite, anorthite and serpentinization. Specially, significant gypsum dissolution was observed at HS05, HS09 and HS14 before and after the earthquake, suggesting that the earthquake broke the balance of water-rock reaction and promoted the dissolution of gypsum. Combined with geological background and previous studies, we propose that shallow sedimentary minerals, such as gypsum, have the potential to be used as earthquake warning indicators. However, shallow minerals are controlled by many external factors (e.g., temperature, pressure, climatic conditions, seasonal changes etc.), which greatly weakens their practical value in earthquake early warning.

https://doi.org/10.5194/hess-2024-395
Preprint. Discussion started: 20 December 2024

Hydrology and Earth System Sciences Open Access
Discussions

Key words: Geothermal fluid; Water-rock interaction; Earthquake forecasting; PHREEQC; Gypsum; East Anatolian Fault Zone.

https://doi.org/10.5194/hess-2024-395
Preprint. Discussion started: 20 December 2024

Hydrology and Earth System Sciences
Discussions

1 Introduction

On February 6, 2023, southeastern Turkey were struck by a series of devastating earthquakes. The two main earthquakes were *Mw* 7.8 *and Mw* 7.6, followed by multiple aftershocks (Including one of *Mw* 6.7 and several earthquakes of greater than *Mw* 4) (Kwiatek et al., 2023; Ni et al., 2023). The main areas affected by these earthquakes include the provinces of Qahraman, Marash and Hatay. According to official statistics, more than 60,000 people have been killed and millions displaced in southern Turkey and northern Syria (Ma et al., 2024; Över et al., 2023; Wang et al., 2023b).

The double earthquakes in February 2023 occurred along the East Anatolian Fault Zone (EAFZ), one of the more seismically active seismic zones in the world (Whitney et al., 2023). There have been many ruinous earthquakes in history (Hubert-Ferrari et al., 2020; Simão et al., 2016; Sparacino et al., 2022; Tan et al., 2008). Research shows that, at present, East Anatolian fault zone has a left-lateral strike-slip rate of ~11 mm/yr (Pousse‐Beltran et al., 2020). Meanwhile, it is accompanied by a certain thrust process, which causes huge stresses at the plate margin. The massive stress release is the main cause of the February 2023 earthquakes (Kwiatek et al., 2023; Ma et al., 2024; Wang et al., 2023b). Before and after earthquakes, obvious macroscopic anomalies were observed in many hot springs (HS04 and HS14) (Fig. S1), which indicates the fact that the geothermal fluid circulation has been disturbed by seismic activity.

As the important medium of seismic monitoring research, geothermal fluids are widely used in the world e.g., (Franchini et al., 2021; King et al., 2006; Luo et al., 2023; Poitrasson et al., 1999; Skelton et al., 2014; Tsunogai and Wakita, 1995; Wang et al.,

https://doi.org/10.5194/hess-2024-395
Preprint. Discussion started: 20 December 2024

2021). Many important theoretical achievements have been made in the direction of earthquake monitoring and early warning. For example: Changes in groundwater chemistry before two consecutive earthquakes in Iceland (Skelton et al., 2014), Precursory Chemical Changes in Ground Water: Kobe Earthquake, Japan (Tsunogai and Wakita, 1995), etc. However, there is a serious problem that the geothermal fluid anomaly index is not universal. In other words, it is difficult to promote and apply in the world (Luo et al., 2023). The fundamental reason is the complexity of geothermal fluid cycle. Exactly, the two earthquakes in February 2023 in Turkey provides an opportunity to explore the relationship between geothermal fluids and earthquakes. Therefore, the geothermal fluids in the EAFZ are systematically studied in this contribution to tracing the origin of geothermal fluid, restore the water-rock interaction process, and evaluate the influence of seismic activity on the geothermal fluid circulation process. This study would help to deepen the understanding of the influence of earthquakes on geothermal fluid, and provide data reference for earthquake monitoring and early warning research.

2 Geologic background

Located at the intersection of Eurasia, Africa and Arabia, Turkey is a complex tectonic collage (Lanari et al., 2023; Simão et al., 2016). Here, the collision between the Arabian and Eurasian plates was an important tectonic process that began in the early Miocene (~ 23 Ma) and continues to the this day (van Hinsbergen et al., 2024). This collision caused plateau uplift, volcanic eruptions, sedimentary basin formation, and large-scale strike-slip faults in eastern Turkey, including the EAFZ (Fig. 1) (Bilim

https://doi.org/10.5194/hess-2024-395
Preprint. Discussion started: 20 December 2024

et al., 2018; Karaoğlu et al., 2018; Karaoğlu et al., 2020; Whitney et al., 2023; Yönlü et al., 2017; Zhou et al., 2024).

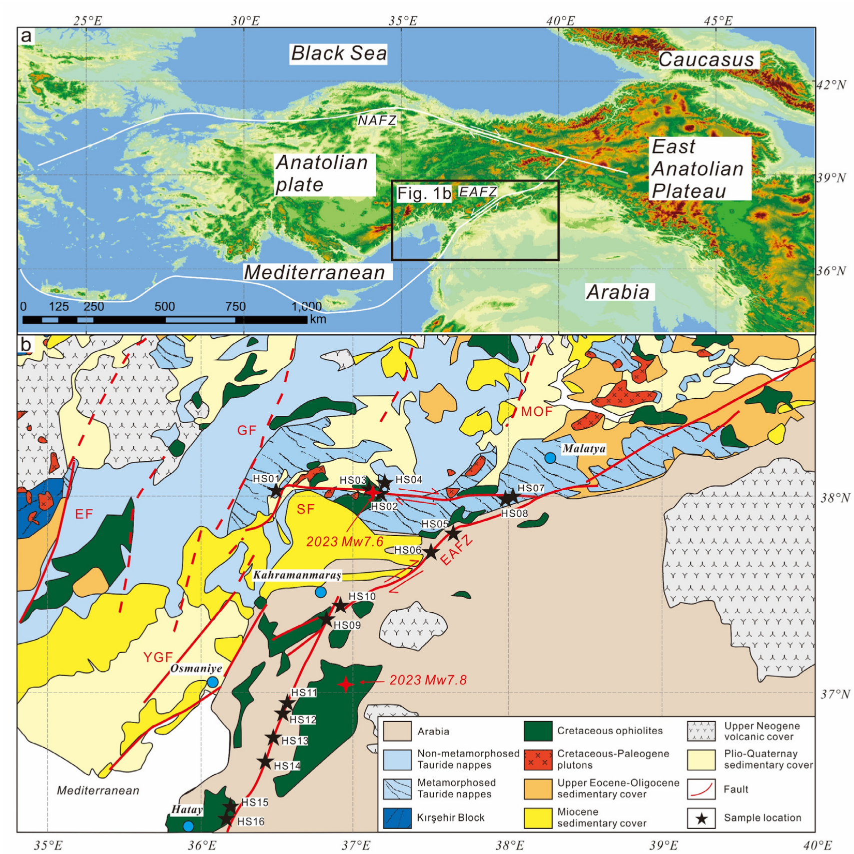

Figure 1. a: A brief Map of the eastern Mediterranean region from NASADEM (https://doi.org/10.5069/G93T9FD9). b: Geological map of EAFZ, modified from (van Hinsbergen et al., 2024). EF: Ecemiş Fault, SF: Sürgü Fault, MOF: Malatya-Ovacık Fault, GF: Göksün Fault, YGF: Yeşilgöz-Göksün Fault.

The formation of the EAFZ is related to the northward subduction of a strong and thin lithospheric wedge under the Arabian Plate (Nalbant et al., 2002; Sparacino et al., 2022). This subduction process led to the formation of a stress concentration zone that

https://doi.org/10.5194/hess-2024-395
Preprint. Discussion started: 20 December 2024

eventually developed into a strike-slip fault that penetrated the entire lithosphere, i.e. the EAFZ (Nalbant et al., 2002). In addition, because the African plate and the Arabian plate are still moving northward, this fault zone is also accompanied by a certain thrust process, which causes huge stresses at the plate margin (Ma et al., 2024; Över et al., 2023; Özkan et al., 2023; Pousse - Beltran et al., 2020; Wang et al., 2023b; Whitney et al., 2023).

The stratigraphic composition of the East Anatolian fault zone is complex, including Non-metamorphosed Tauride nappes and Metamorphosed Tauride nappes crystallization base, Cretaceous ophiolites and Cretaceous-Paleogene plutons. It is overlaid by clastic deposits, lacustrine deposits (such as: Ancient Amik Lake) and volcanic cover of Upper Eocene-Oligocene to Plio-Quaternay. Faults are widely developed in study area, including East Anatolian Fault, Ecemiş Fault, Sürgü Fault, Malatya-Ovacık Fault, Göksün Fault, Yeşilgöz-Göksün Fault etc. (van Hinsbergen et al., 2024). These faults has been active for a long time and has a history of devastating earthquakes, including two in February 2023 (*Mw* 7.8 and *Mw* 7.6) (Fig. 1) (Carena et al., 2023; Kwiatek et al., 2023; Ma et al., 2024; Maden and Öztürk, 2015; Över et al., 2023; Özkan et al., 2023; Pousse - Beltran et al., 2020; Tan et al., 2008; Wang et al., 2023b).

The climate of the EAFZ is mainly a temperate continental climate with cold winters and hot and dry summers. The average annual rainfall is between 200 mm and 600 mm, and is mainly winter rain. Due to its inland location and low rainfall, the flow of the river is relatively small. The groundwater system is relatively complex, and geothermal resources are mainly distributed near the fault zone and its controlled areas, including low or moderate temperature geothermal systems, which have great potential for development and utilization (Aydin et al., 2020; Güleç and Hilton, 2016; Inguaggiato et al., 2016; Karaoğlu et al., 2019).

3 Sampling and analytical methods

16 samples of water were collected in EAFZ, including hot springs, geothermal wells and river water. Detailed sample collection and testing methods can be found at Luo et al. (2023). In short, the water sample was taken with a 50 mL clean polyethylene bottle and the temperature and pH of the water were measured and recorded. Two samples are collected at each sampling site, one is added with ultrapure HNO_3 to analyse the cation content, and the other is used to analyse the anion content and isotopic composition. All samples need to be pre-treated with a 0.45 μm filter membrane to remove impurities before being tested. MAT 253 was used to analyses δD and $\delta^{18}O$ (relative to Vienna Standard Mean Ocean Water (V - SMOW)). The cation and anion were analysed by Dionex ICS-900 ion chromatograph (Thermo Fisher Scientific Inc.). HCO_3^- and CO_3^{2-} was determined by acid-base titration with a ZDJ-100 potentiometric titrator. SiO_2 were analysed by inductively coupled plasma emission spectrometer Optima-5300 DV (PerkinElmer Inc.). Trace elements were analysed by Element XR ICP-MS. Multielement standard solutions (IV-ICPMS 71A, IV-ICP-MS 71B and IV-ICP-MS 71D, iNORGANIC VENTURES) used for quality control (the analytical error margin of major cations and trace elements were less than 10%).

4 Results

Physical, chemical and isotopic compositions of geothermal water are listed in Table 1. The pH of the water samples varied from 7.03 to 11.72, and all the samples showed weakly alkaline characteristics except HS15 (pH=11.72). The effluent temperature of water sample is low (8.1~32°C), and the highest temperature is HS15 well sample (32°C). HS08 is a river sample with the lowest temperature (8.1°C). SiO_2 varies from 0.38 mg/L to 84.64mg/L, and the closer to the epicenter, the higher the SiO_2 content. HCO_3^- (165.72~1854.3 mg/L) is the main anion. The concentration of SO_4^{2-} range from 1.21 mg/L to 316.61 mg/L, and the concentration of SO_4^{2-} in some samples is obviously increased (e.g. HS01, HS03, HS04, HS14). The concentration of Na^+ (0.42~88.93 mg/L), Cl^- (0.97~75.92 mg/L) and B (3.62~1047.25 μg/L) changed synergistically. The Na^+, Cl^- and B content of HS14, HS15 and HS16 increased significantly. Ca^{2+} (14.16~501.58 mg/L) is the main cation, followed by Mg^{2+} (0.38~116.2 mg/L). The types of geothermal water include Na-Cl-HCO_3, Ca-HCO_3, Ca-HCO_3-SO_4 and Mg-HCO_3 (Fig. 2). The $\delta^{18}O$ and δD of samples varied from –11.30‰ to –6.55‰ and –65.43‰ to –34.43‰ respectively, which is near to the global meteoric water line (GMWL) (Craig, 1961) (Fig. 3), suggesting their meteoric water origin.

The composition of trace elements in geothermal fluids are shown in Table 2. The contents of Sr (30.13~3244.88 μg/L) and Ba (1.89~196.48 μg/L) in the samples varied widely. Moreover, Sr and SO_4^{2-} had obvious positive correlation. Statistical analysis shows that the concentration of fluid activity elements, such as B (3.62~1047.25 μg/L), Li (0.33~89.93 μg/L) and Rb (0.14~28.91 μg/L), are at historic highs versus (Fig. S2). Enrichment coefficients (EF) normalized by Ti is used for geothermal fluids and rocks.

The result shows that Whether compared with schist, basalt or Andesite of EAFZ, trace elements in geothermal fluids are all in a state of enrichment, and some elements can even be enriched 100000 times (Fig. S3).

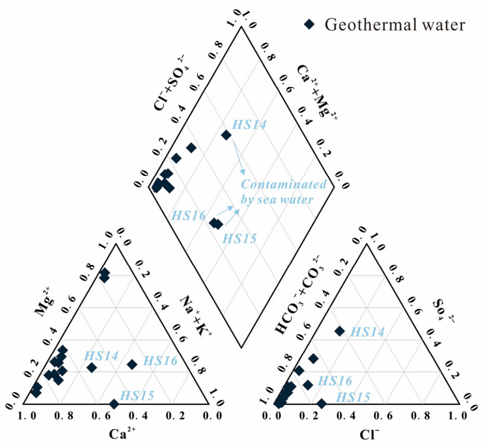

Figure 2. Piper plot of sampled geothermal waters in EAFZ. The geothermal waters are Na-Cl-HCO3, Ca-HCO3, Ca-HCO3-SO4 and Mg-HCO3 types.

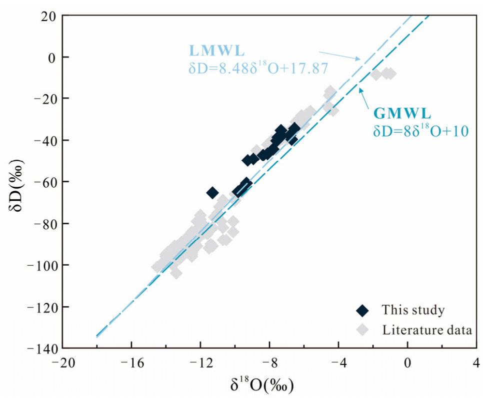

Figure 3. δD and $\delta^{18}O$ (‰V-SMOW) values for geothermal waters collected from EAFZ. The GMWL represents the global meteoric water line (Craig, 1961).

According to this study and literature data (Aydin et al., 2020; Yuce et al., 2014), Local Meteoric Water Line (LMWL) is $\delta D = 8.48\ \delta^{18}O+17.87$ (R^2=0.95, n=110).

https://doi.org/10.5194/hess-2024-395
Preprint. Discussion started: 20 December 2024

Hydrology and Earth System Sciences
Discussions

Table 1.Physical, Chemistry and isotopic compositions of geothermal waters from the EAFZ.

No	Long (E)	lat (N)	Type	Date	T	pH	EC	SiO_2	Li^+	Na^+	K^+	Mg^{2+}	Ca^{2+}	F^-	Cl^-	NO_3^-	SO_4^{2-}	HCO_3^-	$CO3^{2-}$	δD	$\delta^{18}O$
	(°)	(°)			(ºC)		(μS/cm)	(mg/L)	(mg/L)	(mg/L)	(mg/L)	(mg/L)	(mg/L)	(mg/L)	(mg/L)	(mg/L)	(mg/L)	(mg/L)	(mg/L)	(‰)	(‰)
HS01	*36.52*	*38.00*	S	03/22/2024	15.8	8.12	1565	20.7	-	27.93	4.85	75.69	253.85	3.6	55.46	-	287.74	670.01	-	-64.93	-9.81
HS02	*37.17*	*38.03*	S	03/22/2024	13.2	8.35	287	5.27	-	0.42	-	6.58	54.04	0.4	1.33	5.06	6.37	178.53	-	-65.43	-11.30
HS03	*37.17*	*38.03*	S	03/22/2024	13.2	7.12	1876	26.36	0.13	48.44	0.48	74.2	368.42	0.5	30.85	30.13	103.56	1271.1	-	-60.77	-9.33
HS04	*37.17*	*38.03*	S	03/22/2024	15	7.03	2683	84.64	0.05	19.9	0.46	116.2	501.58	3.7	9.29	3.33	229.75	1854.3	-	-63.82	-9.64
HS05	*37.67*	*37.81*	S	03/23/2024	12.7	8.5	634	14.42	-	7.66	0.39	25.88	103.61	0.53	4.43	12.92	29.75	367.72	-	-44.29	-7.79
HS06	*37.51*	*37.70*	S	03/23/2024	15	8.27	774	15.34	-	4.19	0.32	54.08	100.99	0.43	5.98	1.61	7.96	515.66	-	-46.53	-8.11
HS07	*38.06*	*37.94*	S	03/23/2024	9.8	8.46	276	9.41	-	0.84	-	4.62	55.11	0.41	0.97	2.74	5	167.86	-	-49.09	-8.93
HS08	*38.05*	*37.94*	R	03/24/2024	8.1	8.43	275	15.15	-	1.13	-	4.47	55.34	0.44	1.06	3.83	5.69	165.72	-	-49.81	-9.26
HS09	*36.81*	*37.35*	S	03/24/2024	18	8.11	699	25.5	0.01	5.85	0.21	42.6	94.99	0.52	6.8	8.87	93.44	344.96	-	-37.65	-6.81
HS10	*36.99*	*37.46*	S	03/25/2024	20	8.48	659	31.29	-	1.57	-	90.13	18.22	0.35	3.8	7.53	2.76	459.47	-	-39.65	-6.71
HS11	*36.55*	*36.89*	S	03/25/2024	16.3	8.27	517	9.69	-	2.32	0.09	27.89	75.25	0.45	4.39	9.25	12.11	312.24	-	-40.30	-7.58
HS12	*36.52*	*36.81*	S	03/25/2024	16.9	8.32	489	46.5	-	2.11	-	60.76	14.16	0.52	6.13	14.55	4.27	307.98	-	-34.43	-6.55
HS13	*36.44*	*36.67*	S	03/26/2024	18.2	8.22	579	10.05	0.01	4.87	0.49	30.35	81.56	0.5	7.67	8.67	39.89	309.4	-	-37.88	-7.30
HS14	*36.37*	*36.50*	W	03/26/2024	23.5	8.21	1305	36.64	0.09	62.4	5.79	65.12	151.43	4.33	75.92	34.6	316.61	300.15	-	-38.61	-7.51
HS15	*36.16*	*36.38*	S	03/26/2024	32	11.72	589	0.38	0.02	48.64	1.42	0.38	55.55	0.41	48.71	5.28	1.21	-	154.61	-47.27	-8.37
HS16	*36.15*	*36.27*	S	03/27/2024	24.5	8.45	1100	32.57	0.01	88.93	18.68	59.6	73.35	0.72	67.11	43.51	75.9	484.37	-	-35.34	-7.33

Note: “-” represents below detection limit or undetected. “S” is Hot spring, “W” is Well water, “R” is river water.

https://doi.org/10.5194/hess-2024-395
Preprint. Discussion started: 20 December 2024

Hydrology and Earth System Sciences Discussions

Table 2.Trace elements compositions of geothermal waters from the EAFZ.

No	B	Al	P	Sc	Ti	V	Mn	Fe	Co	Ni	Ga	Rb	Sr	Y	Zr	Nb	Ba	Hf	Ta	Pb	Th	U
	(μg/L)	(μg/L)	(μg/L)	(μg/L)	(μg/L)	(μg/L)	(μg/L)	(μg/L)	(μg/L)	(μg/L)	(μg/L)	(μg/L)	(μg/L)	(μg/L)	(μg/L)	(μg/L)	(μg/L)	(μg/L)	(μg/L)	(μg/L)	(μg/L)	(μg/L)
HS01	35.49	10.02	66.41	0.04	0.20	0.23	369.58	34.43	0.40	3.40	0.03	1.68	1231.40	0.04	0.19	0.02	77.45	0.004	0.01	0.19	0.001	3.15
HS02	3.62	8.26	8.94	0.02	0.22	0.85	0.73	21.10	0.01	0.16	0.04	0.25	99.69	0.01	-	0.02	16.12	-	0.01	0.14	-	0.43
HS03	1047.25	8.23	11.86	0.08	0.19	0.56	0.80	23.29	0.03	4.22	0.04	5.95	691.57	0.01	0.01	0.01	5.52	0.001	0.01	0.10	-	1.32
HS04	512.31	6.75	12.88	0.58	0.22	0.19	890.21	563.31	4.06	19.67	0.01	28.91	1505.17	0.12	0.66	0.02	11.28	0.004	0.01	0.13	0.003	0.23
HS05	43.88	6.88	9.14	0.04	0.17	2.23	0.90	16.14	0.04	0.88	0.04	0.31	667.55	0.02	0.03	0.01	196.48	0.001	0.01	0.17	-	1.64
HS06	18.60	4.50	8.79	0.03	0.18	2.74	0.67	13.54	0.02	6.23	0.01	0.37	213.59	0.02	0.03	0.01	38.11	0.001	0.01	0.15	-	0.51
HS07	8.32	12.99	10.51	0.01	0.20	2.09	3.58	81.59	0.02	0.37	0.11	0.49	53.27	0.03	0.01	0.01	3.48	-	0.01	0.26	0.004	0.32
HS08	4.77	12.27	8.89	0.03	0.18	2.85	1.05	12.52	0.02	0.26	0.01	0.44	55.78	0.06	-	0.01	1.89	-	-	0.10	-	0.26
HS09	24.05	8.48	4.56	0.04	0.27	0.50	0.99	45.62	0.01	0.81	0.02	0.62	967.07	0.02	-	0.01	105.53	-	-	0.15	-	0.49
HS10	14.56	8.37	9.74	0.03	0.23	0.73	0.62	19.86	0.02	0.68	0.01	0.19	96.74	0.06	-	-	7.85	-	-	0.16	-	0.02
HS11	9.13	8.17	13.04	0.02	0.18	0.64	2.58	134.71	0.03	2.05	0.01	0.36	263.61	0.02	0.01	0.01	22.37	0.001	-	0.11	-	0.53
HS12	7.37	28.55	23.54	0.03	0.30	1.24	2.51	49.33	0.14	5.73	0.05	0.14	34.78	0.09	-	-	38.75	-	-	0.18	0.001	0.03
HS13	14.94	10.65	10.86	0.02	0.47	0.60	15.09	805.45	0.07	1.27	0.05	0.96	592.95	0.02	0.01	0.01	146.07	-	-	0.17	-	1.01
HS14	183.76	17.48	7.06	0.07	0.14	2.50	2.94	12.72	0.04	11.66	0.00	11.25	3244.88	0.02	0.02	0.01	92.96	0.001	0.01	0.10	0.001	0.34
HS15	4.34	5.41	6.85	0.03	0.19	0.03	0.69	14.15	0.01	0.32	0.00	1.86	30.13	0.01	-	-	2.36	-	-	0.15	-	0.01
HS16	491.19	6.67	812.91	0.03	0.29	7.20	0.89	34.78	0.10	10.68	0.00	2.23	738.82	0.02	0.02	-	39.83	0.001	0.01	0.20	0.002	5.08

Note: "-" represents below detection limit or undetected. Hf and Ta are kept to 3 decimal places due to their low content.

https://doi.org/10.5194/hess-2024-395
Preprint. Discussion started: 20 December 2024

Hydrology and Earth System Sciences Discussions

5 Discussion

5.1 The origin of geothermal fluids

Hydrogen and oxygen isotopes are effective geochemical indexes for tracing the origin of geothermal fluids. It can be seen from Fig. 3 that the hydrogen and oxygen isotopes of the sample have obvious positive correlation. Combined with the geothermal fluid data of EAFZ in the literatures, the correlation between the hydrogen and oxygen isotopes is $\delta D = 8.48\ \delta^{18}O + 17.87$ ($R^2 = 0.95$, n=110), which is consistent with the global meteoric water line (GMWL) (Craig, 1961) (Fig.3), suggesting that these geothermal fluids are controlled by meteoric water. “Oxygen drift” is not obvious, indicating that the degree of water-rock interaction in the geothermal fluid cycle is limited and/or the oxygen isotope composition of the fluid and rock is indiscriminately (However, given the complex and diverse lithology of EAFZ, the latter is highly unlikely) (Fig. 1). The highest value of δD (–6.55‰) and $\delta^{18}O$ (–34.43‰) at the southwest end of EAFZ, which is close to the Mediterranean Sea, indicating that it originates from the recharge of the evaporation of the Mediterranean Sea (Fig.3). Due to the influence of the continent and altitude, the farther away from the coastline, the lighter the hydrogen and oxygen isotopic composition.

Geothermal fields are generally distributed along the EAFZ, which is characterized by low or moderate temperature geothermal systems (Aydin et al., 2020; Baba et al., 2019). Previous studies pointed out that both water and gas characteristics indicate that geothermal fluids is a mixture of shallow and deep components either of mantle and crustal origin (Aydin et al., 2020; Italiano et al., 2013; Yuce et al., 2014).

Yuce et al. (2014) argue that geothermal fluids at the southwest end of the EAFZ are triggered by deep-rooted regional faults. Analogously, there are deep components involved in the geothermal fluid circulation in the middle to east section of EAFZ. However, the source of deep components are thought to be controlled by magmatic activity rather than from deep-rooted regional faults (Aydin et al., 2020; Italiano et al., 2013; Karaoğlu et al., 2019). At the intersection of the EAFZ and the North Anatolian Fault Zones (NAFZ), which is also known as the Karliova triple junction, there is extensive volcanic activity that may have provided energy and components for the geothermal fluid cycle eastern segment of the EAFZ (Bilim et al., 2018; Karaoğlu et al., 2018; Karaoğlu et al., 2020). Furthermore, Italiano et al. (2013) suggested these volcanic activities may even contribute to geothermal fluids in the middle segment of the EAFZ.

Na^+ and Cl^- are often used as a reference when judging whether there is magma mixing in geothermal fluids (Luo et al., 2023; Pan et al., 2021). In the eastern section of EAFZ, the concentration of Na^+ (1.3~2600mg/L) and Cl^- (0.4~2500 mg/L) varies widely (Aydin et al., 2020). In the case of excluding the mixing of halite and seawater (Luo et al., 2023; Wei et al., 2021), it is possible that there is contaminated by magmatic fluid. Petrological and geophysical observations also support magmatic activity in the eastern section of EAFZ (Bilim et al., 2018; Karaoğlu et al., 2018; Karaoğlu et al., 2020; Maden and Öztürk, 2015). Furthermore, Italiano et al. (2013) suggested that $\delta^{13}C_{CO2}$ (–5.6‰~ –0.2‰) and He (Rac (values corrected for the atmospheric contamination) = 0.44~4.41) revealed a fluid of mantle-derived in the middle segment of the EAFZ.

However, the Na^+ (0.42~88.93 mg/L) and Cl^- (0.97~75.92 mg/L) of the samples in this study were both low. HS16, the sample with the highest concentration, was collected at the southwest of EAFZ, which was obviously contaminated by Mediterranean Sea water and had no signal of deep fluid or magma source. This is not consistent with the previous study. Furthermore, the gas and water cycles appear to be decoupled in the EAFZ. We suggest that the reason for the inconsistency may be controlled by two factors: 1) After the earthquake, dislocation movement occurred in the fault zone, resulting in a large amount of surface water and shallow groundwater infiltration, which diluted the geothermal fluid; 2) The origin and evolution of geothermal water and geothermal gas are different. The cycle of geothermal water is essentially a cycle in the upper crust dominated by precipitation and controlled by fault zones. Nevertheless, geothermal gas is dominated by deep fluid, with a little or no air pollution. In addition, the strong fluidity and low density of gas make it easier to removal than water, which makes deep geothermal fluids may not be able to rise along the fault to the shallow crust or surface like geothermal gas. Although there is an obvious signal of deep crust or mantle in geothermal gas, the signal of deep crust or mantle is lacking in geothermal water. Therefore, we argue that the gas and water cycles may be decoupled in the EAFZ, with the gas more responsive to deep information than the water.

Since the deep information is lacking in geothermal water, it can still be used to trace shallow geothermal fluid cycles. Geothermal reservoir temperature estimation is one of the important indicators to understand the geothermal water cycle. We have calculated the thermal reservoir temperature of EAFZ geothermal water, and the results

https://doi.org/10.5194/hess-2024-395
Preprint. Discussion started: 20 December 2024

Hydrology and Earth System Sciences
Discussions

are shown in Table S1. Due to the low water-rock interaction degree and diversity of rock types in this area, cations in water are difficult to reach water-rock equilibrium (Fig. 4). Hence, most of the cationic thermometer estimates are too large or too small, which can only be used as a reference for thermal reservoirs. Fortunately, SiO_2 thermometers are relatively suitable for estimating the reservoir temperature. As can be seen from Table S1, the reservoir temperatures range from 19.81ºC to 128.09 ºC (Quartz, no steam loss), which belongs to the low or moderate temperature geothermal systems. Using the circulation depth calculation formula, the maximum circulation depth is estimated to be 4.4km (HS04) (Table S1). It is very close to the epicenter of the 2023 *Mw* 7.6 earthquake (Fig. 1).

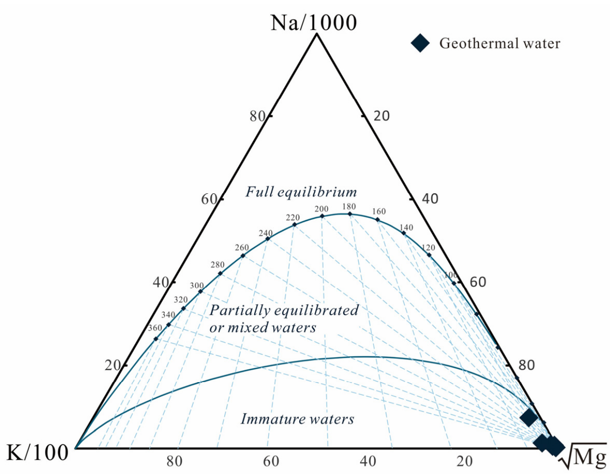

Figure 4. Na-K-Mg ternary diagram of geothermal waters in EAFZ.

As mentioned above, deep geothermal fluid may be diluted by shallow cold water. The silicon-enthalpy model is an effective tool to evaluate and eliminate the effects of the cold water mixing (Fournier, 1977). It can be seen from the Fig. 5a that HS04, which is closest to the epicenter, has the highest reservoir temperature (234 ºC) indicating that

https://doi.org/10.5194/hess-2024-395
Preprint. Discussion started: 20 December 2024

Hydrology and Earth System Sciences
Open Access
Discussions

the earthquake did break the balance of water-rock interaction in the EAFZ and released more deep materials and energy. Furthermore, we applied the Cl^- - enthalpy model to constrain the potential deep geothermal fluid. Fig. 5b suggests that the temperature of the deep geothermal fluid is 382 ºC. Such high temperatures are further evidence of the effect of seismic activity on geothermal fluid circulation.

Therefore, after analysing the data of this study, we suggest that the double earthquakes in February 2023 (*Mw* 7.8 *and Mw* 7.6) modified geothermal fluid in the EAFZ, including: materials and energy. The maximum heat storage temperature and maximum circulation depth of geothermal water are 128 ºC and 4.4km respectively. The temperature of the deep geothermal fluid is 382 ºC. Although the deep fluid modified the geothermal fluid, the geothermal fluid was diluted due to the infiltration of a large amount of shallow cold water after the earthquake, and the information of the deep fluid was eventually occulted.

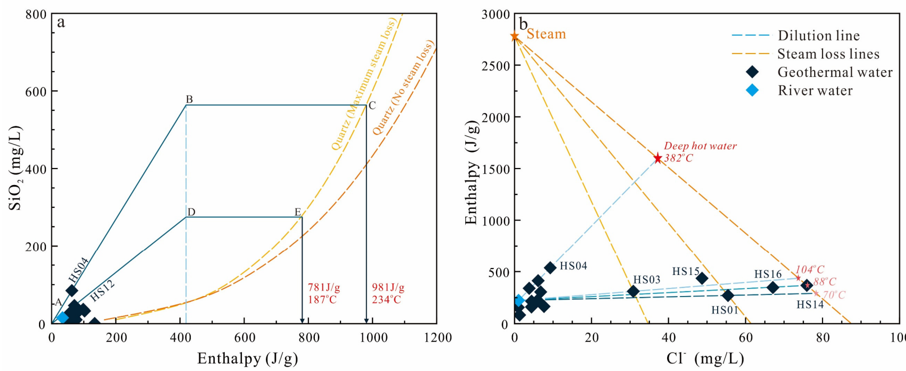

Figure 5. a: Silica-enthalpy model of geothermal waters in LXF zone. b: Enthalpy and Cl^- concentration diagram for identifying the deep hot water in EAFZ. The enthalpies and reservoir temperatures of sample HS04 and HS12 are 981 J/g, 234 ºC and 781

https://doi.org/10.5194/hess-2024-395
Preprint. Discussion started: 20 December 2024

kJ/kg, 187 ºC respectively. Steam point with enthalpy value of 2779.4 J/g and chloride concentration of 0 mg/L (Kretzschmar and Wagner, 2019). The blue diamond is sample HS08, which is river water. HS04 is the closest sampling point to the epicenter, and the temperature of its deep fluid is as high as 382 ºC.

5.2 Water-rocks interaction

As shown in Fig. 3 and 4, the water-rock interaction of the geothermal water is weakly. Nevertheless, we still find chemical composition anomalies in a few samples. Geothermal water samples collected at SF (Sürgü Fault) have higher EC (286.5~2683μs/cm) and ion concentrations, such as Ca^{2+} (54.04~501.58mg/L), Mg^{2+} (6.58~116.20mg/L), and SO_4^{2-} (6.37~287.74mg/L) (Table 1). We arranged the samples collected by EAFZ in the order from northeast to southwest, and the results are shown in Fig. 6. All samples show weak alkalinity (pH=8.11~8.50) except HS15 (pH=11.72). Natural waters with high pH (~ 10 or above) are not usual (Hem, 1985). We suspect that there are two processes that may cause pH to increase: 1) Serpentinization of olivine in ultramafic terranes (Huang; et al., 2023), 2) Secondary mineral precipitation, such as: calcite or magnesite (Aydin et al., 2020; Cipolli et al., 2004). Compared with other samples, the ion concentration of HS15 is significantly reduced, which may indicate the precipitation of potential secondary minerals (e.g., calcite). Therefore, we suggest that process 2 May be the dominant factor leading to the increase of pH.

The Na^{+} and Cl^{-} contents of the samples remained stable and only showed significant positive anomalies near the southwestern end of the Mediterranean Sea, which was caused by seawater pollution (HS14, HS15 and HS16) (Fig. 6d). The low

https://doi.org/10.5194/hess-2024-395
Preprint. Discussion started: 20 December 2024

content and spatial stability of Na^+ (0.84~7.66mg/L) and Cl^- (0.897~7.67mg/L) and the co-variation of hydrogen and oxygen isotopes (Fig. 6c, d), indicating that exogenous Na^+ and Cl^- are not involved in the geothermal water cycle in EAFZ observably (e.g., mantle or magma). In combination with the discussion in section 5.1, we suggest that the low Na^+, Cl^- content is the result of dilution by a large amount of shallow cold water.

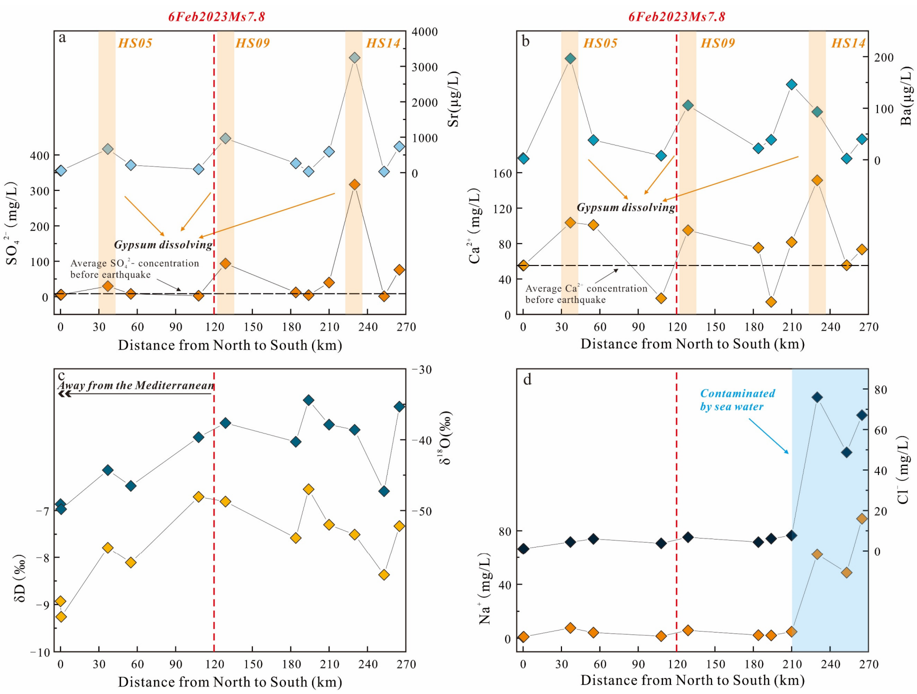

Figure 6. Spatial distribution characteristics of geothermal water in EAFZ after the February 2023 double earthquakes in Turkey. Horizontal coordinate: Starting with the first sample (HS07) at the northeast end, it is distributed in the southwest direction along the EAFZ. From northeast to southwest, they are HS07, 08, 05, 06, 10, 09, 11~16. The number indicates the distance from the HS07 sample. The higher the abscissa, the closer it is to the Mediterranean. Average Ca^{2+} (55.23 mg/L) and SO_4^{2-} (8.31 mg/L) concentrations before earthquake in the EAFZ from Baba et al. (2019).

EAFZ geothermal waters are controlled by shallow circulation. Therefore, the shallow sedimentary cover may be the main factor in the geochemical composition of the modified geothermal waters. We observed positive abnormalities of SO_4^{2-} (2.76~316.61mg/L), Ca^{2+} (14.16~151.43mg/L), Sr (34.78~3244.8μg/L), and Ba (1.89~196.48μg/L) in at least three locations synergistically (HS05, HS09, HS14) (Fig. 6). Apparently, it is due to the dissolution of gypsum. The extensive distribution of evaporative rock layers in EAFZ provides geological evidence for this hypothesis (Aydin et al., 2020; Italiano et al., 2013; Yuce et al., 2014). In particular, HS14 is located near Ancient Amik Lake, and there were macroscopic anomalies such as white water and turbidity before the earthquake, which further verified that the anomalies originated from the dissolution of gypsum (Fig. S1). Furthermore, the Mg^{2+} concentrations of our samples varied from 0.38mg/L to 116.2mg/L, and such a large change may imply the dissolution of Mg-containing minerals, which will be discussed in detail later.

In order to accurately evaluate the cycle process of EAFZ geothermal water, PHREEQC software was used to conduct quantitative simulation of the water-rock interaction process (The simulation calculation process is detailed in Supporting Information) (Parkhurst and Appelo, 2013). The results are shown in Fig. 7. HS05, HS09 and HS14 are consistent with the simulated dissolution curves of 100% gypsum, which confirms our conjecture about the dissolution of gypsum (Fig. 7a). Incidentally, the dissolution curves of celestite ($SrSO_4$) and barite ($BaSO_4$) have also been simulated. HS05 and HS09 may also be affected by the dissolution of barite, while HS14 may also

https://doi.org/10.5194/hess-2024-395
Preprint. Discussion started: 20 December 2024

be affected by the dissolution of celestite (Fig. 7b). HS01, HS03, and HS04 have excessive Ca^{2+} concentrations, indicating that other minerals besides gypsum are involved in the water-rock interaction process and provide Ca (Fig. 7a). After investigating the types of rocks in the study area, we found that in addition to gypsum, other Ca-bearing minerals, such as calcite ($CaCO_3$), dolomite ($CaMg(CO_3)_2$), and Anorthite ($CaAl_2Si_2O_8$), may be involved in the water-rock interaction process. When the ratio of calcite: dolomite : Anorthite = 1:1:1, the simulated results of Ca^{2+} and HCO_3^- are consistent with the observed values, indicating that the three minerals participate in the water-rock interaction in equal proportion (Fig. 7c). Furthermore, HS03 and HS04 have higher ion concentrations than HS01, possibly because HS03 and HS04 are closer to the epicentre of 2023 *Mw* 7.6 earthquake (Fig. 1).

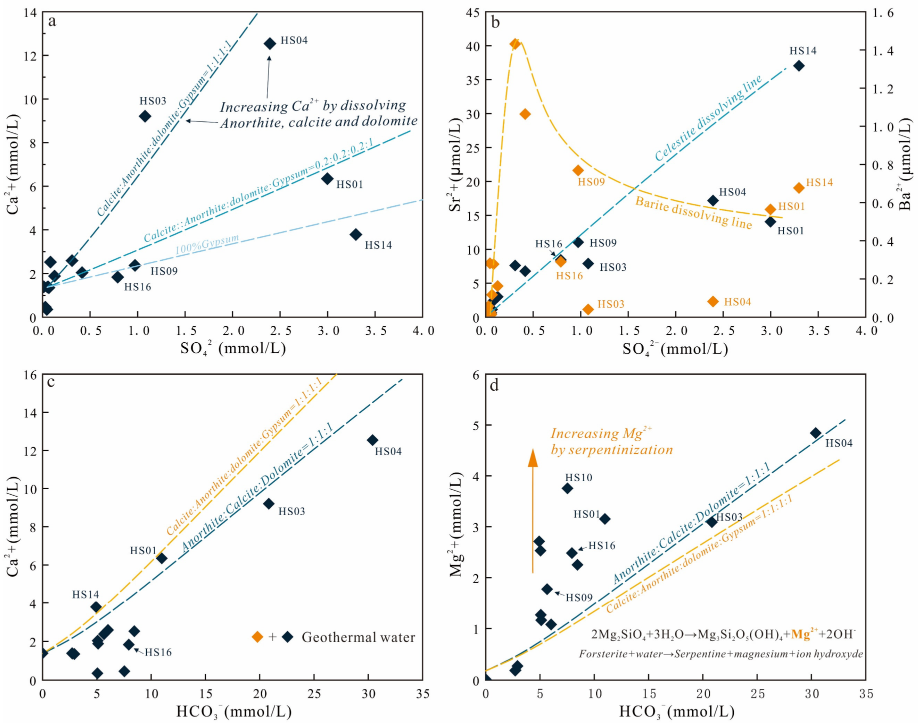

Figure 7. Characteristics of chemical components of geothermal waters in the EAFZ, during water-rock interaction. The diamond is the measured value of geothermal waters. The dashed line is the numerical simulation result of PHREEQC. a: Ca^{2+} vs SO_4^{2-}, b: Sr^{2+} and Ba^{2+} vs SO_4^{2-}, c: Ca^{2+} vs HCO_3^- and d: Mg^{2+} vs HCO_3^-. The simulation calculations are detailed in Supporting Information.

It is worth noting that the Mg^{2+} concentrations in the samples are generally high (0.38~116.2mg/L). It can also be seen from the simulation results that only dolomite provides Mg is not enough to explain the variation of Mg^{2+} concentrations in the sample (Fig. 7d). Actually, considering that the study area is located in the Alpine-Himalayan suture zone, there are a large number of ultrabasic rocks and basic rocks distributed in the region (Fig. 1), which provide the main Mg source for geothermal water (Lanari et al., 2023; Sparacino et al., 2022; van Hinsbergen et al., 2024). Serpentinization of peridotite is the main reason for controlling the variation of Mg content in geothermal water (Fig. 7d) (Aydin et al., 2020; Huang; et al., 2023).

In short, through the analysis of the chemical components of geothermal water and the simulation calculation, we mainly obtained the following understandings: 1) The change of Na^+ and Cl^- concentration in the samples was caused by the mixing of Mediterranean Sea water; 2) Gypsum dissolution exists in geothermal fluids (HS05, HS09 and HS14); 3) Ca^{2+} originated from gypsum, calcite and anorthite; 4) Serpentinization is the main factor controlling Mg^{2+} concentrations.

5.3 Geothermal fluid circulation model in the EAFZ

As discussed above, EAFZ's geothermal fluid circulation model is shown in the Fig. 8. Beginning in the Late Cretaceous, as the New Tethys Ocean closed, Arabia-Eurasia collision zone have accommodated ~350 km of convergence, making crust up to 45 km thick, and causing >2 km of uplift (Yönlü et al., 2017). Arabian lithospheric mantle extends 50~150 km north beneath Anatolian crust (Whitney et al., 2023). Subsequently, the “roll back” and “slab break” occurred, resulting in extensive volcanic and devastating earthquakes, including those of February 6, 2023 in East Anatolian Plateau (Zhou et al., 2024). The collision of the Eurasian and Arabian plates caused Anatolian microplate was extruding westwards, which lead to EAFZ at a high strike-slip rate of ~11 mm/yr (Pousse‐Beltran et al., 2020), and accompanied by counterclockwise rotation with a rotation rate of 1.053 ±0.015°/Ma (Simão et al., 2016). In this tectonic context, EAFZ remains active for a long time. Paleoseismic studies have shown that EAFZ has had many large earthquakes in its history (Carena et al., 2023; Hubert-Ferrari et al., 2020; Sparacino et al., 2022; Tan et al., 2008; Yönlü et al., 2017), with the largest magnitude reaching *Mw* 8.2 (Carena et al., 2023). Fault that cut through the crust provide channels for material and energy to rise up from mantle, which makes EAFZ geothermal gas contain a high proportion of mantle-derived compositions (Aydin et al., 2020; Italiano et al., 2013; Yuce et al., 2014).

However, the transport of geothermal gas and geothermal water appears to be decoupled. On the one hand, deep geothermal fluid stays deep under the influence of gravity and less diffusive, compare to geothermal gas. On the other hand, the geothermal fluid was diluted due to the infiltration of a large amount of shallow cold water after the double earthquakes in February 2023 (*Mw* 7.8 *and Mw* 7.6). Our interpretation can better explain the lack of deep fluid signal in the geothermal water studied in this study. Subsequently, at a depth of 4km, gas-water interaction process was experienced. Finally rose to the surface and discharged into the atmosphere. On the contrary, the circulating geothermal water has undergone complex water-rock interaction processes such as gypsum, calcite, dolomite, anorthite and serpentinization (Fig. 8).

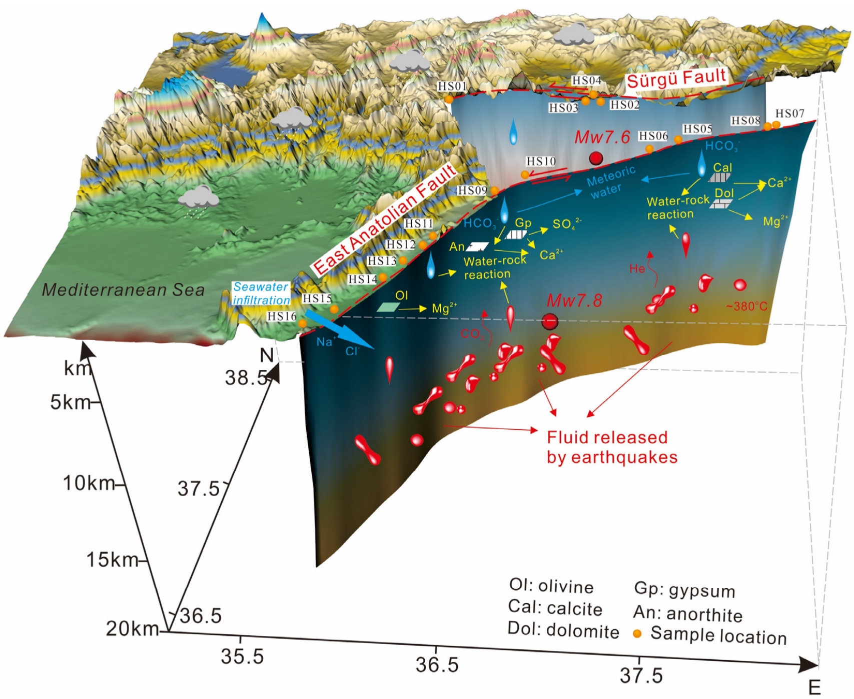

Figure 8. The genesis model of the geothermal fluids in the EAFZ. The deep geothermal fluid was diluted due to the infiltration of a large amount of shallow cold water. In the shallow crust, gas-water interaction process and water-rock interaction processes were experienced. The gases rose to the surface and discharged into the

atmosphere. The circulating geothermal water has undergone complex such as gypsum, calcite, dolomite, anorthite and serpentinization.

5.4 The relationship between geothermal fluid and earthquake forecasting

Earthquake forecasting is a grand goal pursued by human beings, but also one of the most difficult goals. Various physical, chemical and biological techniques are used for earthquake forecasting (Bayrak et al., 2015; Güleç et al., 2002; Kwiatek et al., 2023; Luo et al., 2024; Luo et al., 2023; Miller et al., 2004; Nalbant et al., 2002; Skelton et al., 2014; Tsunogai and Wakita, 1995; Wakita et al., 1980). As a link between the shallow (crust) and the deep (mantle), geothermal fluids can react to various diseases just like human blood. In earlier studies, researchers found that the anomaly of chemical indicators in geothermal fluids could be used for earthquake forecasting e.g., (Güleç et al., 2002; King et al., 2006; Miller et al., 2004; Perez et al., 2008; Poitrasson et al., 1999; Tsunogai and Wakita, 1995), but due to limited technology and funding, such research requiring long-term and large-scale monitoring is difficult to carry out (Ingebritsen and Manga, 2014). With the advancement of technology, more and more automated equipment and the development of 5G communication technology make long-term automatic monitoring possible, e.g., (Barbieri et al., 2021; Boschetti et al., 2022; Franchini et al., 2021; Liang et al., 2023; Luo et al., 2024; Luo et al., 2023; Skelton et al., 2014; Wang et al., 2023a). However, before geothermal fluid is really used in earthquake prediction, there is a problem that must be solved (i.e. to understand the relationship between geothermal fluid and earthquake). Its essence is to restore the origin and evolution process of geothermal fluid (Boschetti et al., 2022).

https://doi.org/10.5194/hess-2024-395
Preprint. Discussion started: 20 December 2024

For a long time, researchers have been searching for the information of the deep fluid in the fault zone, trying to link the earthquake with the deep fluid activity (Liang et al., 2023; Luo et al., 2023; Yan et al., 2024). However, deep information is easily changed during upward migration, and sometimes even lacks deep information, just like the EAFZ geothermal water in this study (Fig. 6d). This seems to limit the ability of geothermal water to be used for earthquake prediction. In fact, chemical anomalies related to seismic activity can still be found in some shallow circulating geothermal water (e.g., SO_4^{2-}) (Luo et al., 2023). Moreover, the shallower water-rock interactions are more sensitive to the environment. Gypsum is widely distributed in nature, and its formation is related to evaporite. Gypsum dissolution and precipitation are often observed in geothermal water. Its solubility is greatly affected by environmental conditions (temperature, pH, pressure etc.) and is a potential indicator of earthquake prediction. After the 2023 *Mw* 7.8 and 2023 *Mw* 7.6 earthquake in EAFZ, in the absence of deep fluid signals, we observed at least three locations of gypsum dissolution, which are likely to have been affected by seismic activity (Fig. 6). Similar SO_4^{2-} anomalies have also been found in the eastern Tibetan Plateau (Li et al., 2021; Luo et al., 2023) and southeast China (Wang et al., 2021). Therefore, we suggest that gypsum can be used as a potential earthquake early warning index, and the synergistic changes of SO_4^{2-}, Ca^{2+}, Sr and Ba may be used as precursor anomalies of earthquakes.

Here, we want to say that although gypsum has the potential to be used for earthquake warning, it is largely affected by climate, rainfall and environmental changes because it is located in the shallow crust. We suggest that the application of

https://doi.org/10.5194/hess-2024-395
Preprint. Discussion started: 20 December 2024

gypsum and other shallow minerals should be treated with caution, and the influence of various factors on the solubility of gypsum should be fully considered. We are urging more detailed work needs to be carried out to improve the theoretical system of the relationship between geothermal fluid and earthquake.

6 Conclusion and Outlook

We have conducted systematic element and isotope analysis on the hydrogeochemistry of geothermal fluid after the earthquake. The geothermal water temperature of EAFZ varies from 8.1°C to 32°C, and the pH changes from 7.03°C to 11.72°C. The types of geothermal water include Na-Cl-HCO_3, Ca-HCO_3, Ca-HCO_3-SO_4 and Mg-HCO_3. The SiO_2 thermometer estimates that the heat storage temperature is 19.81°C to 128.09°C, and the maximum circulation depth is 4.4km. Combined with the geological background, measured data and numerical simulation results, we propose that the geothermal resources of EAFZ is characterized by low or moderate temperature geothermal systems.

In EAFZ, the cycle process of geothermal water and geothermal gas is decoupled. Gravity and large dilution of shallow cold water may be responsible for the water-gas decoupling. The geothermal gas has obvious characteristics of volcanic sources and/or deep-rooted regional faults, while the geothermal water lacks deep fluid signal, which is mainly controlled by the shallow circulation of meteoric waters. SO_4^{2-}, Ca^{2+}, Mg^{2+}, Sr and Ba in geothermal water are obviously affected by water-rock interactions. The water-rock interactions include the dissolution of gypsum, calcite, dolomite, anorthite and serpentinization process.

https://doi.org/10.5194/hess-2024-395
Preprint. Discussion started: 20 December 2024

Hydrology and Earth System Sciences
Open Access
Discussions

Shallow sedimentary minerals, such as gypsum, have the potential to be used as earthquake warning indicators. When earthquakes occur, the changes in the external conditions lead to changes in the solubility of gypsum, which in turn show abnormal concentrations of SO_4^{2-}, Ca^{2+}, Sr and Ba in geothermal water. However, the solubility of gypsum is controlled by many factors (e.g., temperature, pressure, climatic conditions, seasonal changes etc.), which heavily reduces the practical value of gypsum for earthquake early warning.

Code and data availability. All water data are listed in the text or in the Supporting Information.

Supplement. See Supporting Information.

Authorship contributions. **Zebin Luo:** Conceptualization, Methodology, Software, Writing–Original Draft, Writing–Review and Editing. **Xiaocheng Zhou:** Conceptualization, Validation. **Yueren Xu:** Investigation. **Peng Liang:** Investigation. **Huiping Zhang:** Investigation. **Jinlong Liang:** Validation. **Zhaojun Zeng:** Investigation. **Yucong Yan:** Investigation. **Zheng Gong:** Investigation. **Shiguang Wang:** Investigation. **Chuanyou Li:** Investigation. **Zhikun Ren:** Investigation. **Jingxing Yu:** Investigation. **Zifa Ma:** Investigation. **Junjie Li:** Investigation.

Competing Interests. The authors declare that they have no known competing financial interests or personal relationships that could have appeared to influence the work reported in this paper.

Acknowledgements. We would like to thank the Associate Editor and anonymous reviewers for their constructive comments, suggestions and corrections. We also thank

Dr. Yinchun Wang Dr. Renjie Li and Dr. Yi Yu for discussion, Dr. Shiqi Zhang for her help for diagram drawing.

Financial support. The work was funded by National Key Research and Development Project (2024ZD1000503，2023YFC3012005-1), Central Public-interest Scientific Institution Basal Research Fund (CEAIEF20240405, CEAIEF2022030200, CEAIEF2022030205), the National Natural Science Foundation of China (41673106, 4193000170), IGCP Project 724.

https://doi.org/10.5194/hess-2024-395
Preprint. Discussion started: 20 December 2024

Hydrology and Earth System Sciences
Discussions

References

Aydin, H., Karakuş, H., and Mutlu, H.: Hydrogeochemistry of geothermal waters in eastern Turkey: Geochemical and isotopic constraints on water-rock interaction, Journal of Volcanology and Geothermal Research, 390, 2020.

Baba, A., Şaroğlu, F., Akkuş, I., Özel, N., Yeşilnacar, M. İ., Nalbantçılar, M. T., Demir, M. M., Gökçen, G., Arslan, Ş., Dursun, N., Uzelli, T., and Yazdani, H.: Geological and hydrogeochemical properties of geothermal systems in the southeastern region of Turkey, Geothermics, 78, 255-271, 2019.

Barbieri, M., Franchini, S., Barberio, M. D., Billi, A., Boschetti, T., Giansante, L., Gori, F., Jonsson, S., Petitta, M., Skelton, A., and Stockmann, G.: Changes in groundwater trace element concentrations before seismic and volcanic activities in Iceland during 2010-2018, Science of the Total Environment, 793, 2021.

Bayrak, E., Yılmaz, Ş., Softa, M., Türker, T., and Bayrak, Y.: Earthquake hazard analysis for East Anatolian Fault Zone, Turkey, Natural Hazards, 76, 1063-1077, 2015.

Bilim, F., Aydemir, A., Kosaroglu, S., and Bektas, O.: Effects of the Karacadag Volcanic Complex on the thermal structure and geothermal potential of southeast Anatolia, Bulletin of Volcanology, 80, 2018.

Boschetti, T., Barbieri, M., Barberio, M. D., Skelton, A., Stockmann, G., and Toscani, L.: Geothermometry and water-rock interaction modelling at Hafralkur: Possible implications of temperature and CO2 on hydrogeochemical changes previously linked to earthquakes in northern Iceland, Geothermics, 105, 2022.

Carena, S., Friedrich, A. M., Verdecchia, A., Kahle, B., Rieger, S., and Kübler, S.: Identification of Source Faults of Large Earthquakes in the Turkey ‐ Syria Border Region Between 1000 CE and the Present, and Their Relevance for the 2023 Mw 7.8 Pazarcık Earthquake, Tectonics, 42, 2023.

Cipolli, F., Gambardella, B., Marini, L., Ottonello, G., and Zuccolini, M. V.: Geochemistry of high-pH waters from serpentinites of the Gruppo di Voltri (Genova, Italy) and reaction path modeling of CO₂ sequestration in serpentinite aquifers, Applied Geochemistry, 19, 787-802, 2004.

Craig, H.: Isotopic Variations in Meteoric Waters, Science, 133, 1702-1703, 1961.

Fournier, R. O.: Chemical geothermometers and mixing models for geothermal systems, Geothermics, 5, 41-50, 1977.

Franchini, S., Agostini, S., Barberio, M. D., Barbieri, M., Billi, A., Boschetti, T., Pennisi, M., and Petitta, M.: HydroQuakes, central Apennines, Italy: Towards a hydrogeochemical monitoring network for seismic precursors and the hydro-seismo-sensitivity of boron, Journal of Hydrology, 598, 2021.

Güleç, N. and Hilton, D. R.: Turkish geothermal fields as natural analogues of CO 2 storage sites: Gas geochemistry and implications for CO 2 trapping mechanisms, Geothermics, 64, 96-110, 2016.

Güleç, N., Hilton, D. R., and Mutlu, H.: Helium isotope variations in Turkey:: relationship to tectonics, volcanism and recent seismic activities, Chemical Geology, 187, 129-142, 2002.

Hem, J. D.: Study and interpretation of the chemical characteristics of natural water,

https://doi.org/10.5194/hess-2024-395
Preprint. Discussion started: 20 December 2024

Hydrology and Earth System Sciences
Discussions
Open Access

Geological Survey water-supply paper (USA), 2254, 1985.

Huang;, R., Shang;, X., Zhao;, Y., Sun;, W., and Liu;, X.: Effect of Fluid Salinity on Reaction Rate and Molecular Hydrogen (H_2) Formation During Peridotite Serpentinization at 300°C, Journal of Geophysical Research-Solid Earth, 128, e2022JB025218, 2023.

Hubert-Ferrari, A., Lamair, L., Hage, S., Schmidt, S., Çağatay, M. N., and Avşar, U.: A 3800 yr paleoseismic record (Lake Hazar sediments, eastern Turkey): Implications for the East Anatolian Fault seismic cycle, Earth and Planetary Science Letters, 538, 2020.

Ingebritsen, S. E. and Manga, M.: EARTHQUAKES Hydrogeochemical precursors, Nature Geoscience, 7, 697-698, 2014.

Inguaggiato, C., Censi, P., D'Alessandro, W., and Zuddas, P.: Geochemical characterisation of gases along the dead sea rift: Evidences of mantle-co2 degassing, Journal of Volcanology and Geothermal Research, 320, 50-57, 2016.

Italiano, F., Sasmaz, A., Yuce, G., and Okan, O. O.: Thermal fluids along the East Anatolian Fault Zone (EAFZ): Geochemical features and relationships with the tectonic setting, Chemical Geology, 339, 103-114, 2013.

Karaoğlu, Ö., Bazargan, M., Baba, A., and Browning, J.: Thermal fluid circulation around the Karliova triple junction: Geochemical features and volcano-tectonic implications (Eastern Turkey), Geothermics, 81, 168-184, 2019.

Karaoğlu, Ö., Browning, J., Salah, M. K., Elshaafi, A., and Gudmundsson, A.: Depths of magma chambers at three volcanic provinces in the Karlıova region of Eastern Turkey, Bulletin of Volcanology, 80, 2018.

Karaoğlu, Ö., Gülmez, F., Göçmengil, G., Lustrino, M., Di Giuseppe, P., Manetti, P., Savaşçın, M. Y., and Agostini, S.: Petrological evolution of Karlıova-Varto volcanism (Eastern Turkey): Magma genesis in a transtensional triple-junction tectonic setting, Lithos, 364-365, 2020.

King, C.-Y., Zhang, W., and Zhang, Z.: Earthquake-induced Groundwater and Gas Changes, Pure and Applied Geophysics, 163, 633-645, 2006.

Kretzschmar, H.-J. and Wagner, W.: International Steam Tables Properties of Water and Steam based on the Industrial Formulation IAPWS-IF97, Springer Vieweg Berlin, Heidelberg, 2019.

Kwiatek, G., Martinez-Garzon, P., Becker, D., Dresen, G., Cotton, F., Beroza, G. C., Acarel, D., Ergintav, S., and Bohnhoff, M.: Months-long seismicity transients preceding the 2023 M(W) 7.8 Kahramanmaras earthquake, Turkiye, Nat Commun, 14, 7534, 2023.

Lanari, R., Boutoux, A., Faccenna, C., Herman, F., Willett, S. D., and Ballato, P.: Cenozoic exhumation in the Mediterranean and the Middle East, Earth-Science Reviews, 237, 2023.

Li, C., Zhou, X., Yan, Y., Ouyang, S., and Liu, F.: Hydrogeochemical Characteristics of Hot Springs and Their Short-Term Seismic Precursor Anomalies along the Xiaojiang Fault Zone, Southeast Tibet Plateau, Water, 13, 2021.

Liang, J., Yu, Y., Shi, Z., Li, Z., Huang, Y., Song, H., Xu, J., Wang, X., Zhou, X., Huang, L., Luo, Z., Tong, J., and Zhai, W.: Geothermal springs with high δ13CCO2-DIC along the Xianshuihe fault, Western Sichuan, China: A geochemical signature of enhanced deep tectonic activity, Journal of Hydrology, 623, 129760, 2023.

Luo, Z., Yang, M., Zhou, X., Liu, G., Liang, J., Liu, Z., Hua, P., Ma, J., Hu, L., Sun, X., Cui, B., Wang, Z., and Chen, Y.: Evaluation of Various Forms of Geothermal Energy Release in the Beijing Region, China, Water, 16, 2024.

Luo, Z., Zhou, X., He, M., Liang, J., Li, J., Dong, J., Tian, J., Yan, Y., Li, Y., Liu, F., Ouyang, S., Liu, K., Yao, B., Wang, Y., and Zeng, Z.: Earthquakes evoked by lower crustal flow: Evidence from hot spring geochemistry in Lijiang-Xiaojinhe fault, Journal of Hydrology, 619, 129334, 2023.

Ma, Z., Li, C., Jiang, Y., Chen, Y., Yin, X., Aoki, Y., Yun, S. H., and Wei, S.: Space Geodetic Insights to the Dramatic Stress Rotation Induced by the February 2023 Turkey‐Syria Earthquake Doublet, Geophysical Research Letters, 51, 2024.

Maden, N. and Öztürk, S.: Seismic b-Values, Bouguer Gravity and Heat Flow Data Beneath Eastern Anatolia, Turkey: Tectonic Implications, Surveys in Geophysics, 36, 549-570, 2015.

Miller, S. A., Collettini, C., Chiaraluce, L., Cocco, M., Barchi, M., and Kaus, B.: Aftershocks driven by a high-pressure CO2 source at depth, Nature, 427, 724-727, 2004.

Nalbant, S. S., McCloskey, J., Steacy, S., and Barka, A. A.: Stress accumulation and increased seismic risk in eastern Turkey, Earth and Planetary Science Letters, 195, 291-298, 2002.

Ni, S., Sun, H., Somerville, P., Yuen, D. A., Milliner, C., Wang, H., Zhou, J., and Cui, Y.: Complexities of the Turkey-Syria doublet earthquake sequence, Innovation, 4, 2023.

Över, S., Demirci, A., and Özden, S.: Tectonic implications of the February 2023 Earthquakes (Mw7.7, 7.6 and 6.3) in south-eastern Türkiye, Tectonophysics, 866, 2023.

Özkan, A., Solak, H. İ., Tiryakioğlu, İ., Şentürk, M. D., Aktuğ, B., Gezgin, C., Poyraz, F., Duman, H., Masson, F., Uslular, G., Yiğit, C. Ö., and Yavaşoğlu, H. H.: Characterization of the co-seismic pattern and slip distribution of the February 06, 2023, Kahramanmaraş (Turkey) earthquakes (Mw 7.7 and Mw 7.6) with a dense GNSS network, Tectonophysics, 866, 2023.

Pan, S., Kong, Y., Wang, K., Ren, Y., Pang, Z., Zhang, C., Wen, D., Zhang, L., Feng, Q., Zhu, G., and Wang, J.: Magmatic origin of geothermal fluids constrained by geochemical evidence: Implications for the heat source in the northeastern Tibetan Plateau, Journal of Hydrology, 603, 2021.

Parkhurst, D. L. and Appelo, C. A. J.: Description of input and examples for PHREEQC version 3: a computer program for speciation, batch-reaction, one-dimensional transport, and inverse geochemical calculations, U.S. Geological Survey, Reston, VA, 2013.

Perez, N. M., Hernandez, P. A., Igarashi, G., Trujillo, I., Nakai, S., Sumino, H., and Wakita, H.: Searching and detecting earthquake geochemical precursors in CO2-rich groundwaters from Galicia, Spain, Geochemical Journal, 42, 75-83, 2008.

Poitrasson, F., Dundas, S. H., Toutain, J.-P., Munoz, M., and Rigo, A.: Earthquake-related elemental and isotopic lead anomaly in a springwater, Earth and Planetary Science Letters, 169, 269-276, 1999.

Pousse‐Beltran, L., Nissen, E., Bergman, E. A., Cambaz, M. D., Gaudreau, É., Karasözen, E., and Tan, F.: The 2020 Mw 6.8 Elazığ (Turkey) Earthquake Reveals Rupture Behavior of the East Anatolian Fault, Geophysical Research Letters, 47, 2020.

Simão, N. M., Nalbant, S. S., Sunbul, F., and Komec Mutlu, A.: Central and eastern Anatolian crustal deformation rate and velocity fields derived from GPS and earthquake data, Earth and Planetary Science Letters, 433, 89-98, 2016.

Skelton, A., Andren, M., Kristmannsdottir, H., Stockmann, G., Morth, C.-M., Sveinbjoernsdottir, A., Jonsson, S., Sturkell, E., Gudorunardottir, H. R., Hjartarson, H., Siegmund, H., and Kockum, I.: Changes in groundwater chemistry before two consecutive earthquakes in Iceland, Nature Geoscience, 7, 752-756, 2014.

Sparacino, F., Galuzzi, B. G., Palano, M., Segou, M., and Chiarabba, C.: Seismic coupling for the Aegean - Anatolian region, Earth-Science Reviews, 228, 2022.

Tan, O., Tapirdamaz, M. C., and Yoruk, A.: The earthquake catalogues for Turkey, Turkish Journal of Earth Sciences, 17, 405-418, 2008.

Tsunogai, U. and Wakita, H.: Precursory chemical changes in ground water: kobe earthquake, Japan, Science (New York, N.Y.), 269, 61-63, 1995.

van Hinsbergen, D. J. J., Gürer, D., Koç, A., and Lom, N.: Shortening and extrusion in the East Anatolian Plateau: How was Neogene Arabia-Eurasia convergence tectonically accommodated?, Earth and Planetary Science Letters, 641, 2024.

Wakita, H., Nakamura, Y., Kita, I., Fujii, N., and Notsu, K.: Hydrogen release: new indicator of fault activity, Science (New York, N.Y.), 210, 188-190, 1980.

Wang, B., Zhou, X., Zhou, Y., Yan, Y., Li, Y., Ouyang, S., Liu, F., and Zhong, J.: Hydrogeochemistry and Precursory Anomalies in Thermal Springs of Fujian (Southeastern China) Associated with Earthquakes in the Taiwan Strait, Water, 13, 2021.

Wang, Y., Zhou, X., Tian, J., Zhou, J., He, M., Li, J., Dong, J., Yan, Y., Liu, F., Yao, B., Wang, Y., Zeng, Z., Liu, K., Li, L., Li, Z., and Xing, L.: Volatile characteristics and fluxes of He-CO2 systematics in the southeastern Tibetan Plateau: Constraints on regional seismic activities, Journal of Hydrology, 617, 2023a.

Wang, Z., Zhang, W., Taymaz, T., He, Z., Xu, T., and Zhang, Z.: Dynamic Rupture Process of the 2023 Mw 7.8 Kahramanmaraş Earthquake (SE Türkiye): Variable Rupture Speed and Implications for Seismic Hazard, Geophysical Research Letters, 50, 2023b.

Wei, Z.-A., Shao, H., Tang, L., Deng, B., Li, H., and Wang, C.: Hydrogeochemistry and geothermometry of geothermal waters from the Pearl River Delta region, South China, Geothermics, 96, 2021.

Whitney, D. L., Delph, J. R., Thomson, S. N., Beck, S. L., Brocard, G. Y., Cosca, M. A., Darin, M. H., Kaymakci, N., Meijers, M. J. M., Okay, A. I., Rojay, B., Teyssier, C., and Umhoefer, P. J.: Breaking plates: Creation of the East Anatolian fault, the Anatolian plate, and a tectonic escape system, Geology, 51, 673-677, 2023.

Yan, Y., Zhang, Z., Zhou, X., Wang, G., He, M., Tian, J., Dong, J., Li, J., Bai, Y., Zeng, Z., Wang, Y., Yao, B., Xing, G., Cui, S., and Shi, Z.: Geochemical characteristics of hot springs in active fault zones within the northern Sichuan-Yunnan block: Geochemical evidence for tectonic activity, Journal of Hydrology, 635, 2024.

Yönlü, Ö., Altunel, E., and Karabacak, V.: Geological and geomorphological evidence for the southwestern extension of the East Anatolian Fault Zone, Turkey, Earth and Planetary Science Letters, 469, 1-14, 2017.

Yuce, G., Italiano, F., D'Alessandro, W., Yalcin, T. H., Yasin, D. U., Gulbay, A. H.,

Ozyurt, N. N., Rojay, B., Karabacak, V., Bellomo, S., Brusca, L., Yang, T., Fu, C. C., Lai, C. W., Ozacar, A., and Walia, V.: Origin and interactions of fluids circulating over the Amik Basin (Hatay, Turkey) and relationships with the hydrologic, geologic and tectonic settings, Chemical Geology, 388, 23-39, 2014.
Zhou, Z., Thybo, H., Artemieva, I. M., Kusky, T., and Tang, C.-C.: Crustal melting and continent uplift by mafic underplating at convergent boundaries, Nature Communications, 15, 2024.